A Semi-supervised Approach For Brain Tumor Classification Using Wasserstein Generative Adversarial Network with Gradient Penalty

Ashfak Yeafi*, Monira Islam†, Sohag Kumar Mondal‡,
K.M. Ishraq Hussain Nashad§ and Md. Salah Uddin Yusuf¶
Department of Electrical and Electronic Engineering
Khulna University of Engineering & Technology
Khulna-9203, Bangladesh
Email: *yeafiashfak@gmail.com, †monira@eee.kuet.ac.bd, ‡ssohagkumar@gmail.com,
§nashad1803040@stud.kuet.ac.bd, ¶suyusuf@eee.kuet.ac.bd

***Abstract*—Brain tumors represent abnormal growths of brain tissues, contributing significantly to mortality among affected patients globally. The use of various deep learning (DL) networks to improve this diagnostic procedure has been prompted by the development of magnetic resonance imaging (MRI) as a significant tool for the detection of tumors in the brain. However, a persistent challenge in this field arises from the limited availability of appropriately annotated data. This work introduces a semi-supervised DL methodology for brain tumor identification. The proposed approach involves the utilization of a Wasserstein Generative Adversarial Network with Gradient Penalty (WGAN-GP) trained with a mixture of labeled and unlabeled data. As a result, the discriminator of the WGAN-GP efficiently learns robust features and data distribution patterns from instances of data with and without labeling. The trained discriminator is then adapted to perform the classification task. Leveraging pre-trained WGAN-GP weights, the classifier model exhibits a significant improvement in accuracy when compared to the model without pre-training. With the integration of a pre-trained WGAN-GP model, the proposed network architecture achieves an average classification accuracy of 97.00%. To confirm the effectiveness of this approach, comparative analyses with existing methods are conducted, demonstrating its superior performance over the best results achieved by current techniques.**

***Index Terms*—WGAN-GP, Brain MRI, Classification, Deep learning**

I. Introduction

Brain cancer frequently develops as a result of the fast growth of cells within the brain, which is known as a brain tumor. The classification of brain tumors poses challenges due to variations in size, shape, and location within the brain, with examples including glioma, meningioma, and pituitary tumors. Over five years, individuals under the age of 15 exhibited a recovery rate of approximately 75%, while those aged 15 to 39 showed a rate of approximately 72% for diagnosed brain tumors. In the year 2020, a total of 308,102 individuals were identified as having primary central nervous system (CNS) tumors [1]. Convolutional neural networks (CNNs) have shown significant success in various medical imaging tasks, including brain tumor classification from MRI data. These models can directly learn complex features from the images, leading to improved diagnostic accuracy and efficiency. However, the development of robust brain tumor classification models faces challenges due to the scarcity of large-scale, well-annotated datasets [2]. Adequate and accurately labeled data is crucial for effective training of DL models. Insufficient data may result in overfitting and hinder the classifiers' generalization performance. Advancements in classification techniques can aid in identifying brain tumors and subsequently facilitating diagnosis. Recent progress in the image processing area includes the application of Generative Adversarial Networks (GANs), which are DL algorithms. GANs consist of a generator and discriminator, enabling training on diverse datasets, generating high-quality and realistic images, and distinguishing real from fake data. This process not only increases the size of the current dataset but also gives the GAN's discriminator a unique ability—it learns robust features and comprehends patterns of data distribution from data samples. GANs encounter challenges related to mode collapse, instability during training, and problems associated with the vanishing and exploding gradients phenomenon. The WGAN-GP, an improved version of GANs, addresses their limitations by optimizing the loss function. WGAN-GPs are employed in image processing tasks due to their enhanced training stability, meaningful gradients, mode coverage, and improved sample quality. Integrating WGAN-GPs presents an efficient enhancement approach for brain tumor classification. Semi-supervised learning has grown in importance in recent years as a method for classification tasks. Its crucial function in classifying brain tumors resides in its capacity to maximize the use of weakly labeled data, cut costs associated with annotation, and enhance model generalization. This development offers hope for the creation of more precise and affordable diagnostic instruments for the medical field. These are the key points that this paper focuses on:

1) In this study, a semi-supervised deep learning (DL) methodology is introduced for the identification of brain tumors. We have developed a novel WGAN-GPs model

978-1-6654-0906-3/21/$31.00

aimed at mitigating the challenges associated with limited data availability.

2) The WGAN-GPs discriminator, which has been adapted into a pre-trained deep neural network, is fine-tuned with a limited number of labeled MRI scans to improve its performance in tumor-type classification.

The organization of this paper follows the following format: Section II illustrates the recent work in brain tumor classification. Section III contains the material and methods. Section IV explains the experiment and presents the results. Lastly, Section V concludes the paper.

II. Related work

In the following section, a review of several recent studies about the classification of brain tumors is presented.

An approach for finding and categorizing brain tumors that combines InceptionResNetV2 and Random Forest Tree (RFT) within an ensemble architecture was proposed by Gupta et al. [3]. In this approach, the RFT technique is used to accurately categorize various types of brain tumors, while InceptionResNetV2 is a pre-trained model designed specifically for identifying tumors inside MRI data. The integration also uses cyclic generative adversarial networks to aid in the production of synthetic data. In order to detect tumors and classify them, the author attained accuracy rates of 99% and 98%, correspondingly

Tahir et al. [4] looked into various preprocessing methods to enhance classification outcomes. On numerous test sets, they examined the effectiveness of the three techniques—noise reduction, contrast enhancement, and edge detection—individually and in various combinations. They emphasized the benefit of combining different strategies rather than depending on just one. They utilized these techniques and tested the SVM classifier on the Figshare dataset, achieving an 86% accuracy rate.

Ghassemi et al. [5] utilized a combination of GANs and fully connected (FC) layer deployment in a DL network to accurately classify brain tumors from MRI images. The system had got higher performance than another conventional learning system at 93.01% with an induced split which had turned into 95.6% with a random split.

In another paper, Guzmán et al. [6] used the same dataset combined with Fighshare, SARTAJ, and Br35H datasets and InceptionV3 had the best accuracy of around 97.12%. A hybrid network named AlexNet-KNN had been implemented by AlTahhan et al. [7] to classify brain tumors and showed around 97% accuracy with selected image datasets.

III. Material and methods

A. Dataset description

This work utilizes two different datasets. The first dataset is used for generative training and classification models. It combines MRI scans from sources including Br35H, SARTAJ dataset, and figshare. This dataset contains brain scans from individuals with different types of tumors (gliomas, meningiomas, pituitary tumors) as well as healthy subjects, forming four classes. There are 7021 MRI scans in total, with varying quantities for each category. Each scan is available on Kaggle, in JPEG format, with a resolution of 512 by 512 pixels, and labeled with the specific tumor type [8]. The second dataset called the OASIS dataset [9], involves 150 individuals aged 60 to 96, with a total of 373 imaging sessions. Each participant had multiple MRI scans taken over at least a year, with each session containing three to four T1-weighted MRI scans. The dataset is used specifically for generative training purposes. Selected samples from both datasets are illustrated in Fig. 1.

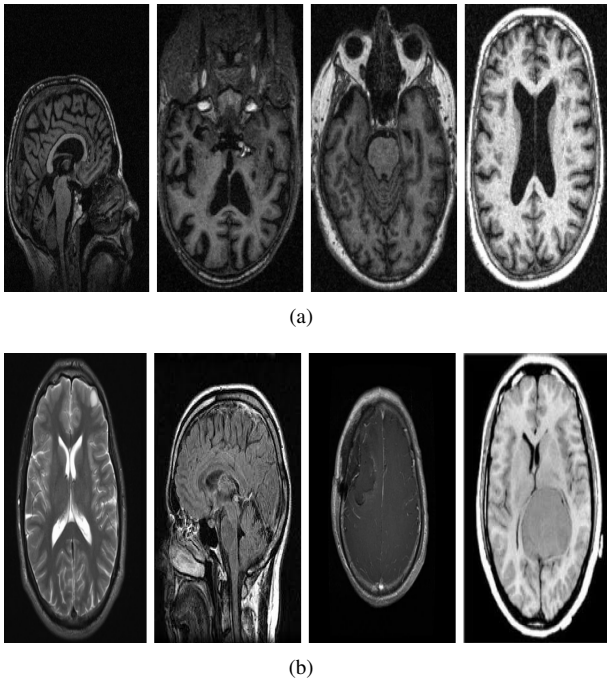

(a)

(b)

Fig. 1. (a) Sample images from OASIS [9] dataset (b) Sample images from Kaggle [8] dataset.

B. Data preprocessing

In traditional methods, preprocessing techniques such as segmentation are often required. However, a study [10] showed that when deep neural networks are applied to MRI pictures, the best results came from doing very little preparation, especially only normalization. To make the analysis easier, the images in this study have been normalized between -1 and 1. For both the WGAN-GP and classifier model the images were resized the images in 128×128. The images in the second data set are volumetric brain scans with a dimensions of $256 * 256 * 128$, resulting in varying dimensions along different axes. Images were square-shaped in the axial perspective before being immediately downsampled to $128 * 128$ dimensions.The other two axes were picked from a specified area of the image, with the second direction having a random size between 128 and 180 pixels and the first direction having 128 pixels. This selected region was then rescaled to achieve a final size of $128 * 128$ pixels. Apart from this, no

data augmentation has been employed in this research paper. In this study, a set of 5709 images from the Kaggle dataset was used for training the classifier model, and a separate subset of 1311 images was isolated for evaluation.

C. Tumor Classification using modified WGAN-GP

The generator G and the discriminator D are the two neural networks that make up the DL architecture known as GAN [11]. The main objective of the discriminator is to determine the origin of a given data point, whether it belongs to a specific database or not. On the other hand, the generator's primary purpose is to produce data points that closely resemble those present in the database, to outsmart the discriminator.

These two neural networks engage in a two-player minimax game: G endeavors to deceive D, leading to an increase in G's score while diminishing D's score. Conversely, D strives to accurately differentiate between real and fake data points, which results in an increase in its score but a decrease in G's score.

$$\min_G \max_D f(D,G) = E_{x\sim P_d}[\log(D(x))] + E_{z\sim P_n}[\log(1-D(G(z)))] \quad (1)$$

The GAN is trained via iterative optimization of the function $f(D,G)$, as denoted in Equation 1. This includes taking into account both the generator G and the discriminator D, where P_d denotes the distribution of actual data, and P_n denotes the distribution of the generator's random vector. While GANs have shown impressive performance, their training stability and convergence have posed challenges. These issues are addressed by the WGAN-GP approach, a variation of the regular GAN [12]. In order to more accurately compare the distributions of actual and produced data, WGAN-GP uses the Wasserstein distance, commonly known as the Earth Mover's Distance (EMD). It gives the discriminator a Lipschitz continuity constraint, improving training stability and preventing issues like mode collapse. The WGAN-GP approach incorporates the Wasserstein distance and gradient penalty, making the training more efficient and generating higher-quality data. This is achieved through the Kantorovich-Rubinstein duality, as expressed in the following equation:

$$\min_G \max_{D\in d} \mathbb{E}_{x\sim P_r}[D(x)] - \mathbb{E}_{\tilde{x}\sim P_g}[D(\tilde{x})] \quad (2)$$

Where d represents a 1-Lipschitz function set, P_g represents the model distribution implicitly defined by P_r, the data distribution. An automated brain tumor classification and detection technique was employed using the WGAN-GP algorithm in this research work. Initially, the MRI datasets underwent uniform data pre-processing steps. Subsequently, the processed MRI images were amalgamated and employed for training the WGAN-GP model. The overall workflow of this paper is illustrated in Fig. 2.

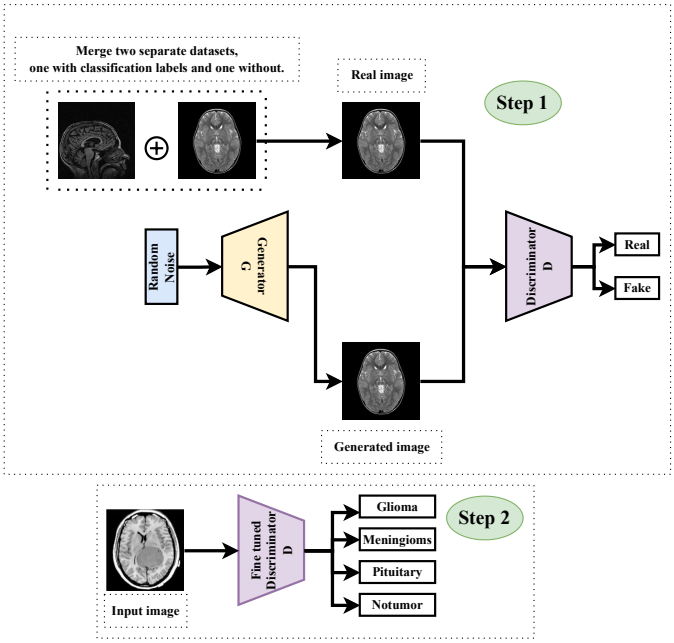

Fig. 2. First two different types of MRI datasets are merged regardless of classification labels and trained into the WGAN-GP model (step 1). The discriminator is adjusted and utilized as a pre-trained model for classifying brain tumors after WGAN-GP training (step 2).

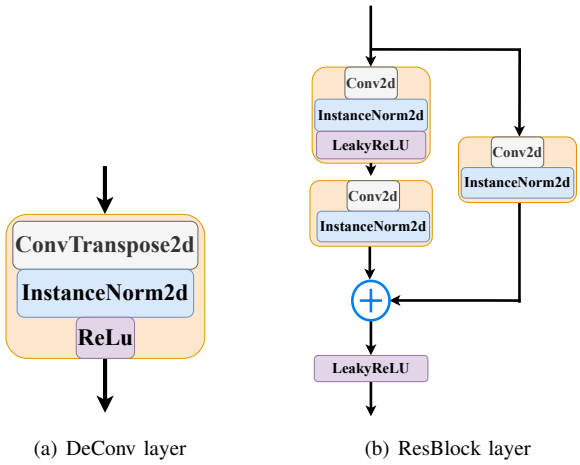

(a) DeConv layer (b) ResBlock layer

Fig. 3. (a) Building structure of DeConv layer (b) Building structure of ResBlock layer.

A 100-dimensional vector-size random noise was utilized as input for the generator. The generator is composed of six consecutive DeConv blocks. Transpose-convolution, instance normalization, and ReLU activation layers are the sequences in which the first five DeConv blocks are implemented. The final DeConv layer only comprises a transpose-convolution layer. Instance normalization is used as an alternative to batch normalization due to the latter's tendency to introduce correlations among images within the same batch [13]. The structure of the DeConv layer is illustrated in Fig. 3(a).

A filter with a $4*4$ kernel size, a stride of 2, and zero padding is used for DeConv1. This initial deconvolutional layer is of paramount importance in the up-sampling process, as it governs the reconstruction of higher-resolution feature maps from the encoded representations.Then, a consistent $4*4$ sized kernel, a stride of 2, and a padding of 1 are used for

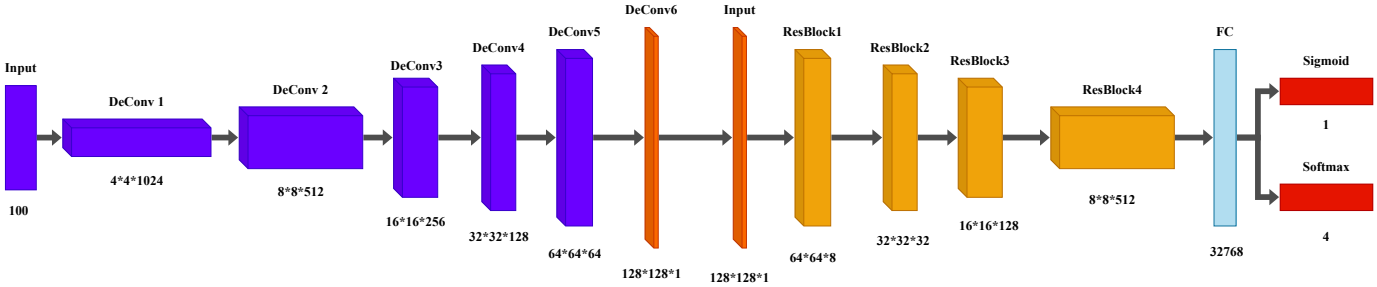

Fig. 4. Overall proposed model architecture.

DeConv2 to DeConv6. These consistent configurations ensure a controlled and efficient up-sampling process throughout the network.

The discriminator receives a $128 * 128$ image as its output after being processed by the generator.

In this research paper, a novel discriminator model is introduced to enhance feature extraction capabilities. The proposed discriminator architecture is made up of four ResBlock layers that are placed one after another, then an FC layer and a sigmoid or softmax layer. Each ResBlock layer consists of CNN, instance normalization, and LeakyRelU activation layers. The structure of the ResBlock layer is illustrated in Fig. 3(b). We incorporate skip connections within the ResBlock layer. The rationale behind employing skip connections stems from their ability to facilitate the seamless flow of information and gradients throughout the network. By enabling direct pathways, skip connections aid in preserving crucial information and gradients that may otherwise encounter loss or dilution when traversing multiple layers [14].

Each ResBlock is characterized by two sequential CNN layers, each featuring distinct kernel sizes, strides, and padding configurations. The first layer has a kernel size of $3 * 3$, a stride of 2, and a padding of 1, whereas the second layer has a kernel size of 1, a stride of 1, and no padding. Notably, a bypass convolutional layer with a kernel size of 1, a stride of 2, and zero padding, is included into the ResBlock to enable the construction of skip connections. With this strategy, the discriminator will be able to understand the structural properties of MRI pictures and extract strong features that are unique to MRI scans.

Following that, the pre-trained CNN is enhanced further to function as a classifier for reliably categorizing brain tumors. This refinement process entails training the CNN on a sizable dataset. The WGAN-GP discriminator's final FC layer is swapped out for a softmax layer during this training phase to facilitate effective classification tasks. Fig. 4 illustrates the proposed architecture of this paper.

IV. EXPERIMENT AND RESULT

A. Experimental setup

An NVIDIA GeForce RTX 4070 Ti GPU and a 13th Gen Intel Core (R) i9-13900K 3.00 GHz CPU were used in the experimental configuration. The DL models were implemented using Python's PyTorch package. The WGAN-GP network underwent training for 500 iterations, employing a batch size of 128. For optimization, the Rmsprop [15] optimizer, as recommended in the original WGAN-GP paper [16], was used for both the generator and discriminator models, with a learning rate of 0.0002. Subsequently, the classifier model underwent training for 50 iterations with 128 batches, utilizing the 0.00005 learning rate of the Adam optimizer for classifier optimization.

B. Result analysis

1) WGAN-GP model: Fig. 5 shows the WGAN-GP's training loss curve, showing that the generator and discriminator losses are approaching zero. Discriminator loss is growing,

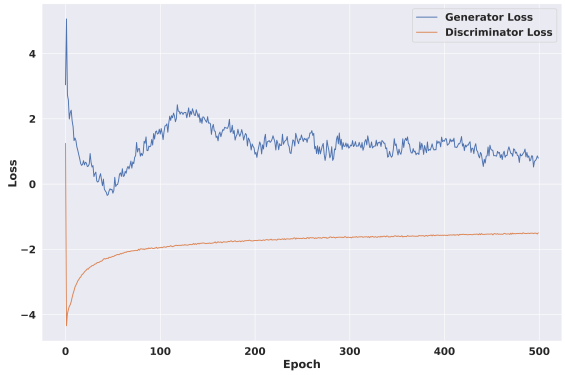

Fig. 5. WGAN-GP model's training loss curve.

while the generator loss is decreasing, according to the loss curve. This shows that both the generator's capacity to create images that cannot be differentiated from real ones and the discriminator's ability to differentiate between created and actual images are becoming better. Additionally, Fig. 6 presents a selection of generator-generated images, which closely resemble real MRI images.

2) Classifier model: To assess the efficacy of the classifier model and enable comparative analysis, a series of metrics have been employed. The computed metrics encompass Ac-

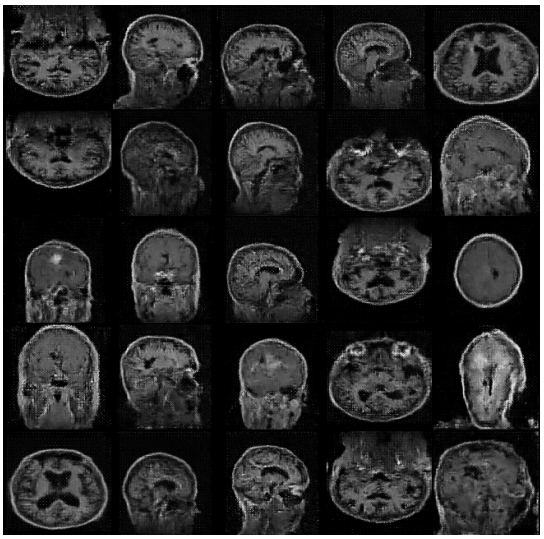

Fig. 6. Generated images by the WGAN-GPs generator.

TABLE I
RESULTS OBTAINED WITHOUT THE USE OF A WGAN PRE-TRAINER

Class	Precision	Recall	F1 score
Glioma	0.91	0.87	0.89
Meningioma	0.84	0.71	0.77
Notumor	0.88	0.99	0.93
Pituitary	0.95	0.97	0.96

curacy, Precision, Recall, F1 score, and the Confusion Matrix. The explicit formula for each metric is elucidated hereafter.

$$Accuracy = \frac{TP+TN}{TP+TN+FP+FN}$$

$$Precision = \frac{TP}{TP+FP}$$

$$Recall = \frac{TP}{TP+FN}$$

$$F1 = \frac{2*Precision*Recall}{Precision+Recall} = \frac{2*TP}{2*TP+FP+FN}$$

where the symbols TP, FN, FP, and TN stand for the corresponding numbers of true positives, false negatives, false positives, and true negatives.

Table II showcases the classification results achieved through the utilization of the WGAN-GP pre-trained model, while Table I illustrates the outcomes obtained when the model was not pre-trained. After evaluating the pre-trained model on test data we have obtained precision values of 96%, 95%, 98%, and 99% for Class Glioma, Class Meningioma, Class Notoumoar, and Pituitary, respectively. This yields average precision and accuracy of 97% and 97%, respectively.

Moreover, Fig. 7 visually represents the impact of the pre-trained model on the learning pace. The results unequivocally demonstrate that the WGAP-GP model has a notable and beneficial effect on the speed at which learning occurs.

TABLE II
RESULTS OBTAINED WITH THE USE OF A WGAN-GP PRE-TRAINER

Class	Precision	Recall	F1 score
Glioma	0.96	0.95	0.96
Meningioma	0.95	0.94	0.95
Notumor	0.98	1.00	0.99
Pituitary	0.99	0.99	0.99

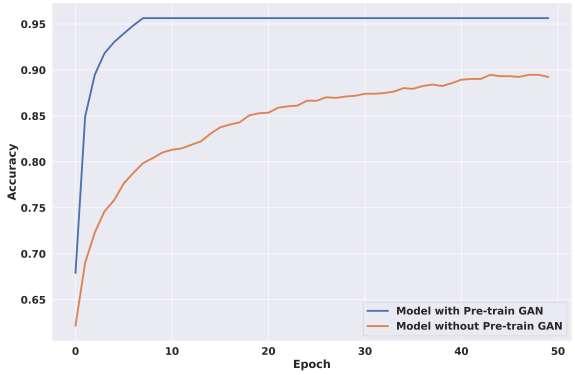

Fig. 7. Comparing the Impact of WGAN-GP Pre-training on Learning Rate Progression.

The confusion matrix for the classification task was visualized in Fig. 8. Each cell in the matrix's intensity indicates the frequency or proportion of samples sorted into certain classifications. The matrix's color gradient highlights categorization distribution, with a strong diagonal suggesting accurate classifications and off-diagonal parts exposing probable mistakes. This heatmap is a useful tool for analyzing model performance and discovering predictive models.

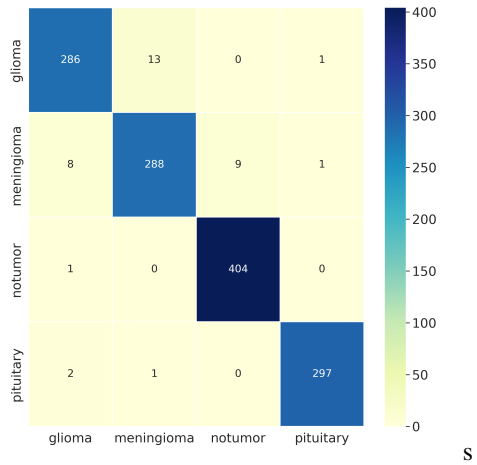

Fig. 8. Confusion matrix of Classifier model.

Upon thorough analysis of the data presented in Table III, it is clear that when compared to other models, the performance of the proposed model is comparable in terms of accuracy, recall, and F1 score.

TABLE III
COMPARISON ANALYSIS WITH OTHER PAPERS

Methods	Precision	Recall	F1 score
GoogLeNet [17]	0.94	0.96	0.95
DCGAN [5]	0. 95	0.94	0.95
Dense CNN [18]	0.96	0.96	0.96
Proposed WGAN-GP	**0.97**	**0.97**	**0.97**

V. CONCLUSION

In conclusion, this work suggests a novel semi-supervised DL approach for brain tumor detection using WGAN-GP. This technique addresses the problem of scarce labeled data and shows promising results by efficiently using unlabeled as well as labeled data. The pre-trained WGAN-GP weights significantly enhance the accuracy of the classifier model, further affirming the efficacy of this approach. The experimental comparisons with existing techniques highlight the superior performance of this proposed methodology, underscoring its potential to advance brain tumor identification and ultimately contribute to improved patient outcomes.

REFERENCES

[1] "Brain tumor: Statistics, https://www.cancer.net/cancer-types/brain-tumor/statistics." [Online]. Available: https://www.cancer.org/cancer/brain-spinal-cord-tumors-adults/about/key-statistics.html

[2] G. Litjens, T. Kooi, B. E. Bejnordi, A. A. A. Setio, F. Ciompi, M. Ghafoorian, J. A. Van Der Laak, B. Van Ginneken, and C. I. Sánchez, "A survey on deep learning in medical image analysis," *Medical image analysis*, vol. 42, pp. 60–88, 2017.

[3] R. K. Gupta, S. Bharti, N. Kunhare, Y. Sahu, and N. Pathik, "Brain tumor detection and classification using cycle generative adversarial networks," *Interdisciplinary Sciences: Computational Life Sciences*, vol. 14, no. 2, pp. 485–502, 2022.

[4] B. Tahir, S. Iqbal, M. Usman Ghani Khan, T. Saba, Z. Mehmood, A. Anjum, and T. Mahmood, "Feature enhancement framework for brain tumor segmentation and classification," *Microscopy research and technique*, vol. 82, no. 6, pp. 803–811, 2019.

[5] N. Ghassemi, A. Shoeibi, and M. Rouhani, "Deep neural network with generative adversarial networks pre-training for brain tumor classification based on mr images," *Biomedical Signal Processing and Control*, vol. 57, p. 101678, 2020.

[6] M. A. Gómez-Guzmán, L. Jiménez-Beristaín, E. E. García-Guerrero, O. R. López-Bonilla, U. J. Tamayo-Perez, J. J. Esqueda-Elizondo, K. Palomino-Vizcaino, and E. Inzunza-González, "Classifying brain tumors on magnetic resonance imaging by using convolutional neural networks," *Electronics*, vol. 12, no. 4, p. 955, 2023.

[7] F. E. AlTahhan, G. A. Khouqeer, S. Saadi, A. Elgarayhi, and M. Sallah, "Refined automatic brain tumor classification using hybrid convolutional neural networks for mri scans," *Diagnostics*, vol. 13, no. 5, p. 864, 2023.

[8] M. Nickparvar, "Brain tumor mri dataset," 2021. [Online]. Available: https://www.kaggle.com/dsv/2645886

[9] D. S. Marcus, A. F. Fotenos, J. G. Csernansky, J. C. Morris, and R. L. Buckner, "Open access series of imaging studies: longitudinal mri data in nondemented and demented older adults," *Journal of cognitive neuroscience*, vol. 22, no. 12, pp. 2677–2684, 2010.

[10] J. S. Paul, A. J. Plassard, B. A. Landman, and D. Fabbri, "Deep learning for brain tumor classification," in *Medical Imaging 2017: Biomedical Applications in Molecular, Structural, and Functional Imaging*, vol. 10137. SPIE, 2017, pp. 253–268.

[11] A. Creswell, T. White, V. Dumoulin, K. Arulkumaran, B. Sengupta, and A. A. Bharath, "Generative adversarial networks: An overview," *IEEE signal processing magazine*, vol. 35, no. 1, pp. 53–65, 2018.

[12] I. Gulrajani, F. Ahmed, M. Arjovsky, V. Dumoulin, and A. C. Courville, "Improved training of wasserstein gans," *Advances in neural information processing systems*, vol. 30, 2017.

[13] S. Xiang and H. Li, "On the effects of batch and weight normalization in generative adversarial networks," *arXiv preprint arXiv:1704.03971*, 2017.

[14] K. He, X. Zhang, S. Ren, and J. Sun, "Deep residual learning for image recognition," in *Proceedings of the IEEE conference on computer vision and pattern recognition*, 2016, pp. 770–778.

[15] G. Hinton, N. Srivastava, and K. Swersky, "Neural networks for machine learning lecture 6a overview of mini-batch gradient descent," *Cited on*, vol. 14, no. 8, p. 2, 2012.

[16] M. Arjovsky, S. Chintala, and L. Bottou, "Wasserstein generative adversarial networks," in *International conference on machine learning*. PMLR, 2017, pp. 214–223.

[17] S. Deepak and P. Ameer, "Brain tumor classification using deep cnn features via transfer learning," *Computers in biology and medicine*, vol. 111, p. 103345, 2019.

[18] O. Özkaraca, O. İ. Bağrıaçık, H. Gürüler, F. Khan, J. Hussain, J. Khan, and U. e. Laila, "Multiple brain tumor classification with dense cnn architecture using brain mri images," *Life*, vol. 13, no. 2, p. 349, 2023.